

Genome-wide transcriptome analysis identifies novel gene signatures implicated in human chronic liver disease

Rana L. Smalling,¹ Don A. Delker,¹ Yuxia Zhang,¹ Natalia Nieto,² Michael S. McGuiness,¹ Shuanghu Liu,¹ Scott L. Friedman,² Curt H. Hagedorn,¹ and Li Wang¹

¹Department of Medicine and Huntsman Cancer Institute, University of Utah School of Medicine, Salt Lake City, Utah; and ²Division of Liver Diseases, Department of Medicine, Mount Sinai School of Medicine, New York, New York

Submitted 13 March 2013; accepted in final form 20 June 2013

Smalling RL, Delker DA, Zhang Y, Nieto N, McGuiness MS, Liu S, Friedman SL, Hagedorn CH, Wang L. Genome-wide transcriptome analysis identifies novel gene signatures implicated in human chronic liver disease. *Am J Physiol Gastrointest Liver Physiol* 305: G364–G374, 2013. First published June 27, 2013; doi:10.1152/ajpgi.00077.2013.—The molecular mechanisms behind human liver disease progression to cirrhosis remain elusive. Nuclear receptor small heterodimer partner (SHP/Nr0b2) is a hepatic tumor suppressor and a critical regulator of liver function. SHP expression is diminished in human cirrhotic livers, suggesting a regulatory role in human liver diseases. The goal of this study was to identify novel SHP-regulated genes that are involved in the development and progression of chronic liver disease. To achieve this, we conducted the first comprehensive RNA sequencing (RNA-seq) analysis of *Shp*^{-/-} mice, compared the results with human hepatitis C cirrhosis RNA-seq and nonalcoholic steatohepatitis (NASH) microarray datasets, and verified novel results in human liver biospecimens. This approach revealed new gene signatures associated with chronic liver disease and regulated by SHP. Several genes were selected for validation of physiological relevance based on their marked upregulation, novelty with regard to liver function, and involvement in gene pathways related to liver disease. These genes include peptidoglycan recognition protein 2, dual specific phosphatase-4, tetraspanin 4, thrombospondin 1, and SPARC-related modular calcium binding protein-2, which were validated by qPCR analysis of 126 human liver specimens, including steatosis, fibrosis, and NASH, alcohol and hepatitis C cirrhosis, and in mouse models of liver inflammation and injury. This RNA-seq analysis identifies new genes that are regulated by the nuclear receptor SHP and implicated in the molecular pathogenesis of human chronic liver diseases. The results provide valuable transcriptome information for characterizing mechanisms of these diseases.

ribonucleic acid sequencing; gene expression; human chronic liver diseases; small heterodimer partner; knockout mice; chronic hepatitis C virus

NONALCOHOLIC FATTY LIVER disease (NAFLD) is the leading cause of chronic liver disease in both children and adults (40). The NAFLD spectrum ranges from simple steatosis (fatty liver) to nonalcoholic steatohepatitis (NASH), which can lead to cirrhosis and hepatocellular carcinoma (HCC) (3, 28, 44). Worldwide, chronic hepatitis C virus (HCV) is another major cause of cirrhosis and HCC (33, 39). Although the risk factors are known, the molecular mechanisms for the progression of liver disease to cirrhosis remain largely undiscovered. The ability to identify specific gene and gene pathway changes that drive progression of chronic liver disease to cirrhosis using state-of-the-art sequencing analysis of human biospecimens

and relevant animal models should be invaluable in developing new preventative, diagnostic, and therapeutic strategies.

This study uses mice deficient in orphan nuclear receptor small heterodimer partner (SHP), officially known as nuclear receptor subfamily 0, group B, member 2 (*Nr0b2*), as a model to investigate genomic changes involved in chronic liver disease development and progression. SHP represses multiple genes involved in hepatic lipid metabolism and inflammation (6, 26, 27, 47) and has been shown to be critical for liver functions, including bile acid synthesis (42). SHP is functionally implicated in cholestatic liver injury due to bile acid feeding (41) or bile duct ligation (34), fatty liver (15, 16), liver fibrosis (46), and liver cancer (50). In addition, SHP is a newly identified regulator of hepatocyte apoptosis (48) and DNA methylation (45, 49). More importantly, SHP levels are downregulated in human cirrhosis (46) and HCC (12). This makes SHP-deficient (*Nr0b2*^{-/-}; referred to as *Shp*^{-/-}) mice, which spontaneously develop hepatoma (50), a suitable model to identify and study molecular mechanisms leading to chronic liver disease and HCC. Recent studies suggest that SHP modulates hepatitis B virus biosynthesis through different nuclear receptors in human Huh7 and HepG2 hepatoma cells (31), but its role in HCV replication has not been explored. However, bile acid receptor farnesoid X receptor, a transactivator of SHP, is involved in HCV replication (38), indicating potential regulation of HCV by SHP as well.

RNA sequencing (RNA-seq) is a comprehensive means of measuring gene expression that provides more detailed information than gene arrays. Analyzing 5'-capped RNA using RNA-seq methods has been shown to be more sensitive than analyzing poly(A)-selected RNA, since it detects mRNAs with short or absent 3'-ends, detects more differentially expressed genes (DEGs), and identifies unannotated Pol II RNAs (33). We used this approach to identify DEGs that may be regulated by SHP and play a role in the development of chronic liver disease. We identified gene expression changes in *Shp*^{-/-} mouse liver using RNA-seq analysis and investigated the enrichment of this signature in chronic hepatitis C cirrhosis and NASH liver biospecimens (2), respectively.

Our analysis identified novel and distinct patterns of gene expression changes that were common to *Shp*^{-/-} mice, hepatitis C cirrhosis, and/or NASH livers relative to controls. These changes were verified by analyzing a large collection of human liver biospecimens, including steatosis, fibrosis, NASH cirrhosis, alcohol cirrhosis, and hepatitis C cirrhosis, as well as mouse models of liver injury and inflammation. Our study identifies novel genes whose expression levels are altered in several major chronic liver diseases and that show physiologically relevant responses to liver injury and inflammation. The

Address for reprint requests and other correspondence: L. Wang, Dept. of Medicine and Huntsman Cancer Institute, Univ. of Utah School of Medicine, Salt Lake City, Utah, 84132 (e-mail: l.wang@hsc.utah.edu).

involvement of these genes in chronic liver disease pathogenesis warrants further detailed investigation.

Glossary

BDL	Bile duct ligation
CCl ₄	Carbon tetrachloride
Cyp2a5	Cytochrome P-450, family 2, subfamily a, polypeptide 5
DAVID	The Database for Annotation, Visualization and Integrated Discovery
DDC	3,5-Diethoxycarbonyl-1,4-dihydrocollidine
DEGs	Differentially expressed genes
DNMT1	DNA methyltransferase 1
DUSP4	Dual specific phosphatase-4
Egr-1	Early growth response 1
FDR	False discovery rate
FXR	Farnesoid X receptor
GO	Gene ontology
Cyp7a1	Cholesterol 7 α -hydroxylase
HCC	Hepatocellular carcinoma
HCV	Hepatitis C virus
KEGG	Kyoto Encyclopedia of Genes and Genomes
MAPK	Mitogen activated protein kinase
MIAME	Minimum Information about a Microarray Experiment
Mmd2	Monocyte to macrophage differentiation-associated 2
NAFLD	Nonalcoholic fatty liver disease
NASH	Nonalcoholic steatohepatitis
PGLYRP2	Peptidoglycan-recognition protein 2
RNA-seq	RNA sequencing
SHP	Small heterodimer partner (nuclear receptor subfamily 0, group B, member 2, <i>Nr0B2</i>)
SMOC2	SPARC-related modular calcium binding protein-2
THBS1	Thrombospondin 1
TSPAN4	Tetraspanin 4
Vaspin	Visceral adipose tissue derived serine protease inhibitor
WT	Wild type

MATERIALS AND METHODS

Animals and human liver samples. *Shp*^{-/-} mice were generated as previously described (42). Briefly, the livers of 8-wk-old male *Shp*^{-/-} mice on a C57BL/6 background and wild-type (WT) C57BL/6 mice fed a normal chow diet were harvested at 12:00 noon, when SHP/*Nr0B2* gene expression is lowest because of its circadian rhythm (32). Total RNA was used for RNA-seq and qPCR ($n = 3$ mice/genotype).

Experimental fibrosis was induced in 2-mo-old male B6129SF2/J mice. Briefly, mice were challenged with CCl₄ (10% vol/vol in corn oil, 5 μ l/g body wt ip two times a week) for 6 wk, or mice were fed a 0.1% 3,5-diethoxycarbonyl-1,4-dihydrocollidine (DDC)-supplemented diet for 6 wk. Whole liver lysates were analyzed. Experimental inflammation was induced by low and high doses of lipopolysaccharide (LPS) in primary hepatocytes according to an established protocol (18). Hepatocytes were isolated from WT and *Shp*^{-/-} mice following our published method (15).

Alcohol-induced liver injury and isolation of hepatic stellate cells. Hepatic stellate cells (HSC) from ethanol-treated rats were generated as described (5). Rats (300 g female Sprague-Dawley, $n = 10$ /group) were fed the control or ethanol Lieber-DeCarli diets for 8 mo (23). Animals received humane care according to the criteria outlined in the

Guide for Care and Use of Laboratory Animals. Details regarding pathology of the liver of the control and alcohol-fed rats are described (5). Animal care and use protocols were approved by the Institutional Animal Care and Use Committee at the University of Utah and Mount Sinai School of Medicine.

The human biospecimens were obtained from liver explants taken during the time of surgery from patients with hepatitis C cirrhosis, alcohol cirrhosis, NASH cirrhosis and fibrosis, and donor livers histologically diagnosed with fibrosis, steatosis, or as normal livers. The biometric and diagnostic details for the human liver specimens procured via the Liver Tissue Cell Distribution System (Minneapolis, MN) are described in supporting documents (data not shown). Procurement and use of additional hepatitis C cirrhosis and normal samples under Institutional Review Board approval has been previously described (33).

RNA isolation and RNA-seq. Total and 5'-capped RNA was purified from mouse and human liver biospecimens as previously described (4). For RNA-Seq of *Shp*^{-/-} mice, the quality of RNA and the PCR libraries used for RNA-seq were as previously described (5), and single 36-bp reads were obtained using the Illumina RNA-seq protocol (30, 33).

qRT-PCR and immunohistochemistry validation. cDNA was prepared from total RNA and reverse transcribed as previously described (46). Primers were designed to qPCR amplify 70- to 200-bp regions of selected genes that were highly differentially expressed in *Shp*^{-/-} mice and hepatitis C cirrhosis and/or NASH. Sequences are available on request. Thermal cycling was carried out using a Roche Light Cycler 480 (Roche Applied Science). The Student's unpaired *t*-test was used in data analysis; $P < 0.05$ was considered significant. Error bars represent the SE of the mean. Gene signatures were validated by qPCR in a subset of human liver specimens and mouse models of liver fibrosis and inflammation.

Sections for immunohistochemistry (IHC) were prepared from snap-frozen human liver tissue specimens fixed in optimum cutting temperature compound. Detection of dual specific phosphatase-4 (DUSP4) protein levels was carried out using a DUSP4 mouse monoclonal antibody (SAB1403748-100UG; Sigma-Aldrich). Immunofluorescent labeling was done using Alexa Fluor 594 Goat Anti-Mouse IgG (H+L) from Life Technologies (A-11005). Sections were counterstained with ProLong Gold Antifade Reagent with DAPI.

Bioinformatics. RNA-seq reads were aligned to the July 2007 mouse reference sequence genome (GRCm37/mm9) for the *Shp*^{-/-} mice ($n = 3$) (GEO accession no.: GSE43893) and the February 2009 human reference sequence genome (GRCh37/hg19) for hepatitis C cirrhosis ($n = 6$) using the Novalign short-read alignment software (36). Sample reads were visualized, and DEGs were identified as previously described (29, 33). The NASH dataset ($n = 7$) was prepared on the GE Healthcare Gene Expression Bioarrays (Codelink) platform (GEO accession no.: GSE17470). The data used were Minimum Information about a Microarray Experiment compliant (2). Genes with a log-transformed false discovery rate (FDR) of >13 (i.e., an untransformed FDR of <0.05 or 5 false positives/100 observations) and greater than or equal to ± 1.5 normalized fold change in expression relative to controls were considered significantly differentially expressed (33). We normalized the log-transformed reads of the DEGs to the average of the controls within each dataset and then used these values to produce hierarchical clustering and generate heat maps of the genes. Enrichment of the *Shp*^{-/-} gene signature in HCV cirrhosis and NASH datasets was statistically determined using Fisher's exact test to generate the two-sided *P* value and the hypergeometric distribution statistic.

Pathway analysis. The Database for Annotation, Visualization, and Integrated Discovery (DAVID) software (13, 14) was used to identify pathways that were differentially altered in *Shp*^{-/-} mice, hepatitis C cirrhosis, and NASH datasets. Briefly, we queried the DEG lists against the human and mouse genome for hepatitis C cirrhosis and NASH, and *Shp*^{-/-} mice, respectively, to generate functional annotations of the gene sets. Kyoto Encyclopedia of Genes and Genomes

(KEGG) and Gene Ontology (GO) pathways that were enriched at a significance level of $P \leq 0.05$ were selected. Individual GO pathways were combined into groups based on functional similarity and common genes.

RESULTS

RNA-seq analysis identifies and predicts SHP-regulated genes. RNA-seq analysis of *Shp*^{-/-} mice serves as an efficient approach to identify and predict genes regulated by SHP. In the *Shp*^{-/-} mice, SHP (*Nr0b2*) exon 1 was replaced as described (42); therefore, sequencing reads were not observed in exon 1 (Fig. 1A) but reads were observed flanking the exon. The analysis of 5'-capped RNA detects both spliced and unspliced isoforms. Therefore, some mRNA transcripts may have been generated from an alternative promoter, but no functional SHP mRNA has been detected in *Shp*^{-/-} mice (42).

Early growth response 1 (*Egr-1*), a SHP-repressed target we recently identified (46), was highly upregulated in *Shp*^{-/-} mice (Fig. 1B) as was mitogen-activated protein kinase (MAPK) pathway activator monocyte-to-macrophage differentiation-associated 2 (19), which suggests it is repressed by SHP (Fig. 1C). Cholesterol 7 α -hydroxylase (*Cyp7a1*), an enzyme of bile acid biosynthesis known to be repressed by SHP (42, 47), was highly overexpressed in *Shp*^{-/-} compared with the WT mice (Fig. 1D). The adipocytokine *Serpina12* (or vaspin, visceral adipose tissue-derived serine protease inhibitor) is increased in NAFLD (1). This gene was decreased in *Shp*^{-/-} mice (Fig. 1E), which are resistant to high cholesterol diet-induced fatty liver (15). Similarly, cytochrome P-450, family 2, subfamily a, polypeptide 5 (*Cyp2a5*), which is induced in xenobiotic-induced hepatotoxicity

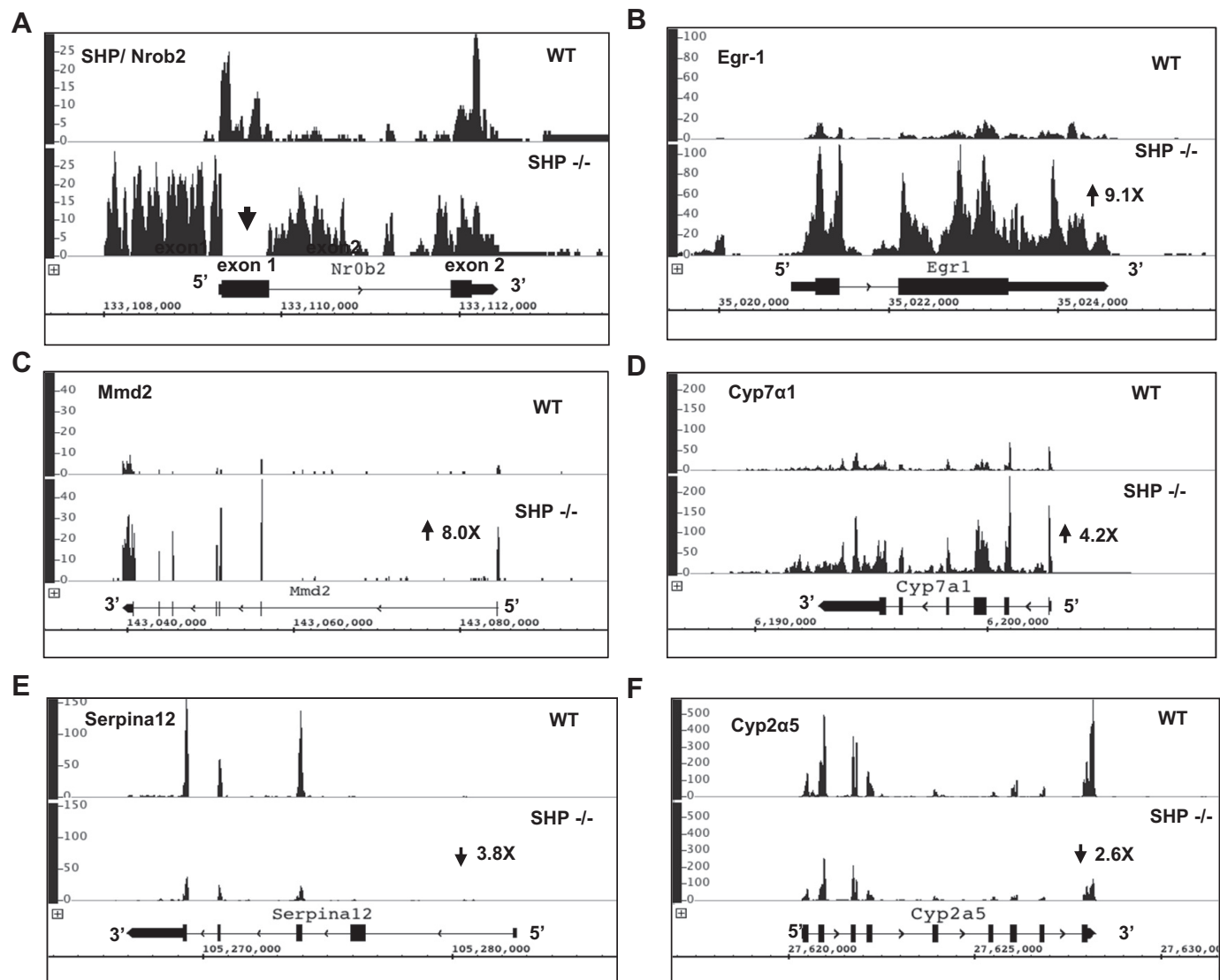


Fig. 1. Identification of novel candidate small heterodimer partner (SHP)-regulated genes by RNA sequencing (RNA-seq) analysis of wild-type (WT) and *Shp*^{-/-} liver. A: Integrated Genome Brower visualization tracks from RNA-seq reads depict complete loss of SHP [nuclear receptor subfamily 0, group B, member 2 (*Nr0b2*)] exon 1 expression in *Shp*^{-/-} mice. B: known SHP target early growth response 1 (*Egr-1*) is increased 9.1-fold in *Shp*^{-/-} mice compared with WT. C: potential SHP target monocyte-to-macrophage differentiation-associated 2 (*Mmd2*) shows a dramatic 8.0-fold increase above WT *Mmd2* levels. D: cholesterol 7 α -hydroxylase (*Cyp7a1*) shows 4.2-fold increased expression in *Shp*^{-/-} mice compared with WT mice. E: expression of *Serpina12* is decreased 3.8-fold in *Shp*^{-/-} mice compared with WT across exons 3, 4, and 5'. F: cytochrome P-450, family 2, subfamily a, polypeptide 5 (*Cyp2a5*) is decreased 2.6-fold in *Shp*^{-/-} compared with WT mice.

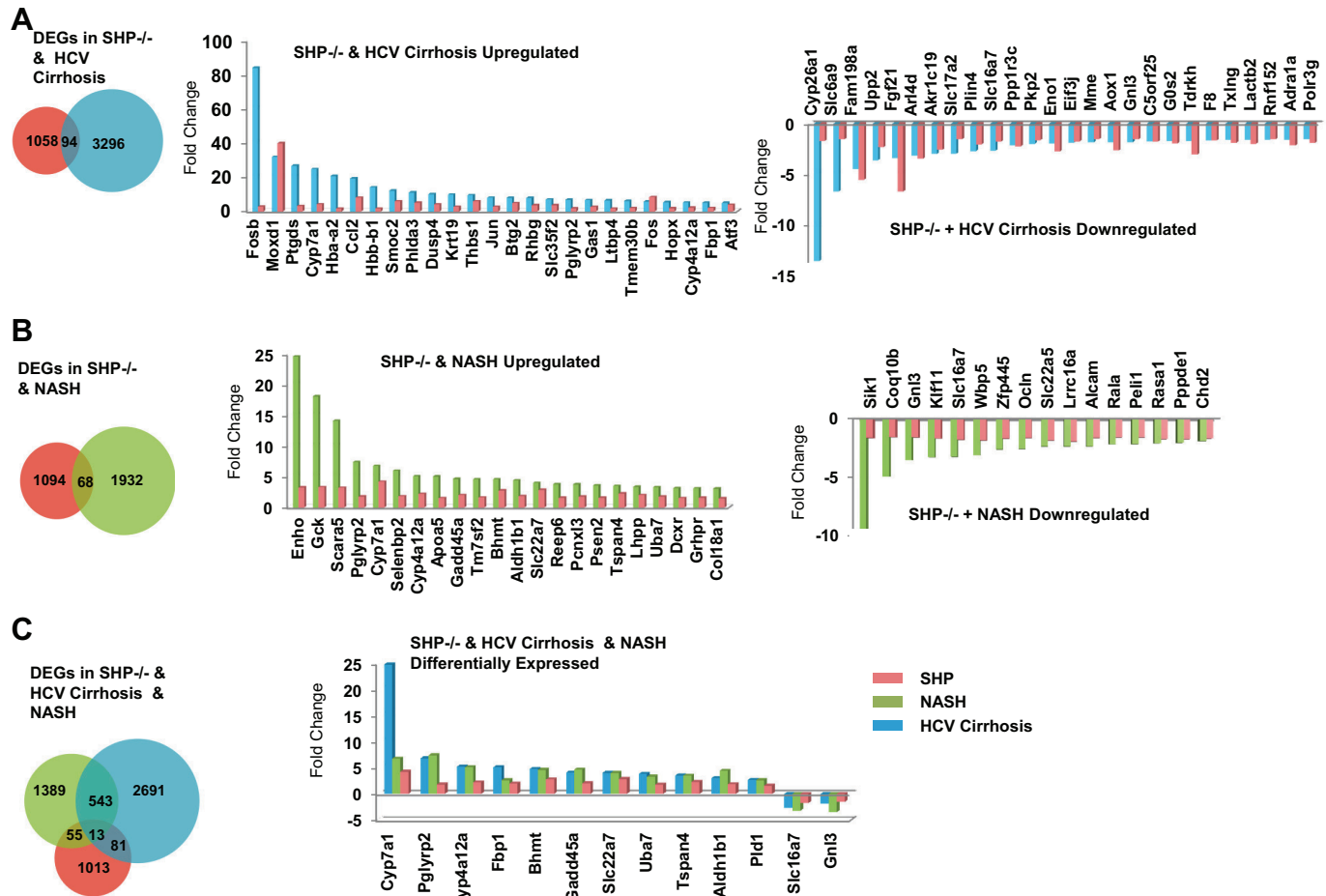


Fig. 2. Unique and common differentially expressed genes (DEGs) in *SHP*^{-/-} mice, nonalcoholic steatohepatitis (NASH), and cirrhotic livers. *A*: Venn diagram shows total numbers and overlapping DEGs between *SHP*^{-/-} mice and hepatitis C cirrhosis (HCV cirrhosis) (*left*). The histograms show the most highly upregulated (*middle*) and downregulated (*right*) genes common in *Shp*^{-/-} and HCV cirrhosis ($P = 0.0011$, hypergeometric distribution = 0.0002). *B*: Venn diagram shows total numbers and common DEGs in both *Shp*^{-/-} mice and NASH (*left*) ($P = 1.919E-006$, hypergeometric distribution = 4.288E-007). The histograms show differentially upregulated (*middle*) and commonly downregulated (*right*) genes in *Shp*^{-/-} and NASH. *C*: *left*, Venn diagram showing total numbers of genes in the three groups and amount commonly downregulated in all of *Shp*^{-/-}, HCV cirrhosis, and NASH. *Right*, histogram identifying those DEGs common across all three datasets, both upregulated and downregulated in HCV cirrhosis, *Shp*^{-/-}, and NASH.

and microbial hepatitis (21), was significantly downregulated (Fig. 1*F*). *Cyp2a5* and *Serpina12* represent genes that are likely activated by SHP through transcription-independent mechanisms. Our approach consistently identifies known SHP-regulated genes, and we subsequently demonstrate its utility in predicting new SHP targets.

Bioinformatics analysis identifies DEGs common to *Shp*^{-/-} mice, hepatitis C cirrhosis, and NASH. The bioinformatics analysis methods and statistical criteria applied to the RNA-seq and microarray data allowed rigorous identification of DEGs in *Shp*^{-/-} mice, NASH, and hepatitis C cirrhosis. We identified 1,161 DEGs in *Shp*^{-/-} mice, 93 of which were enriched in the set of 3,326 genes differentially expressed in hepatitis C cirrhosis ($P = 0.0011$) (Fig. 2A, *left*), and 68 were enriched in the 2,050 DEGs in NASH ($P = 1.919E-006$) (Fig. 2B, *left*). Sixty seven genes were significantly upregulated in hepatitis C cirrhosis and *Shp*^{-/-} mice, whereas 26 were commonly downregulated below 1.5-fold; 25 were upregulated above 5-fold in hepatitis C cirrhosis (Fig. 2A, *middle* and *right*). *Shp*^{-/-} mice and NASH shared 52 upregulated genes; 22 were upregulated above 3-fold in NASH, and 16 were downregulated below

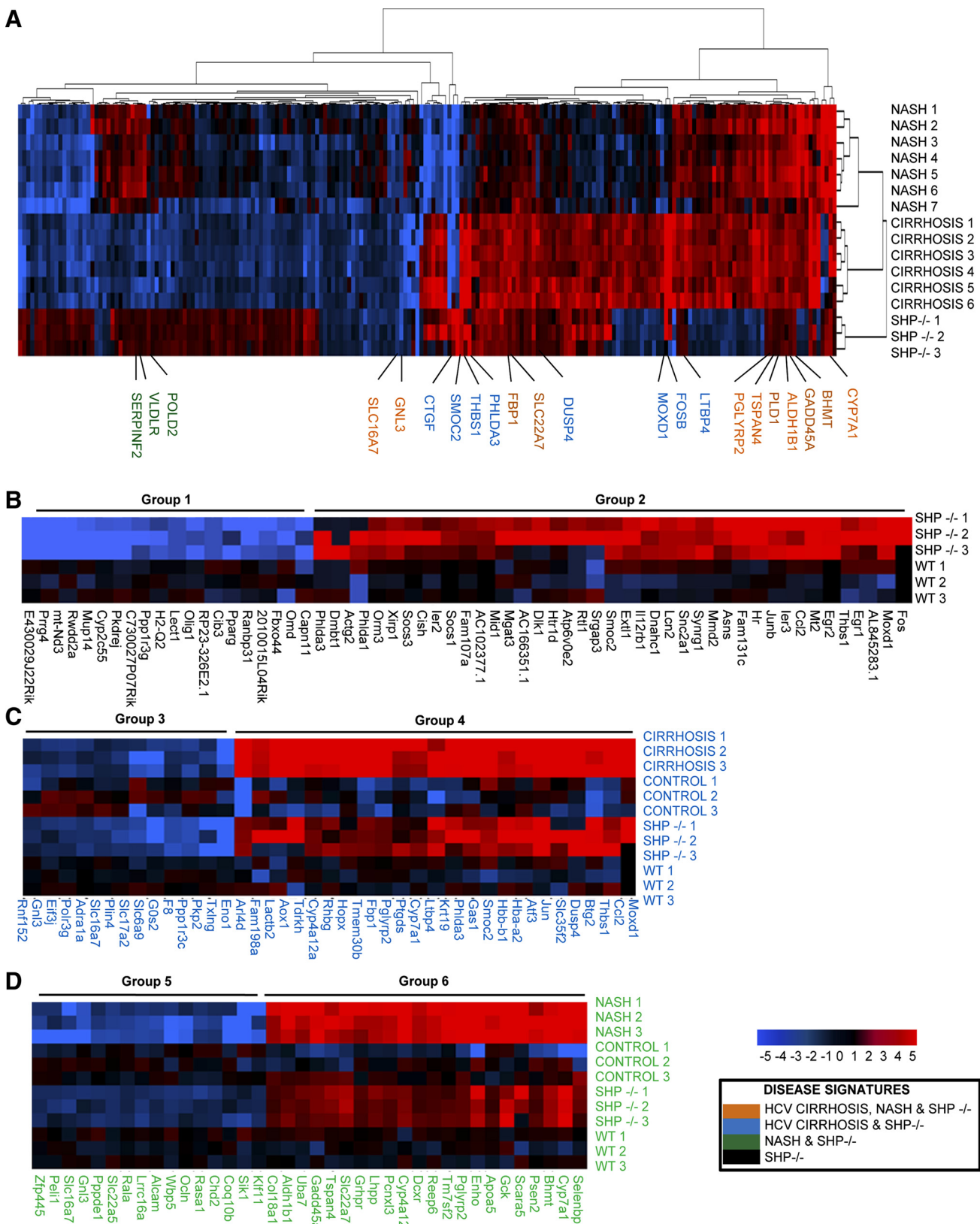
1.5-fold (Fig. 2B, *middle* and *right*). Notably, 13 genes had a similar differential expression pattern in all three conditions (Fig. 2C), suggesting that these genes may play important roles in the development of NASH and cirrhosis and may serve as biomarkers for the presence of these diseases. The fold changes and number of DEGs in hepatitis C cirrhosis and NASH were consistently higher than those for the same genes in *Shp*^{-/-} mice. This likely reflects the greater accumulation of genomic changes over time in the disease states compared with early changes in 2-mo-old *Shp*^{-/-} mice.

Hierarchical clustering reveals shared gene signatures in *Shp*^{-/-} mice, chronic hepatitis C cirrhosis, and NASH. Unsupervised hierarchical clustering of all the genes common to NASH, hepatitis C cirrhosis, and *Shp*^{-/-} mice datasets (Fig. 3A) demonstrated clear up- and downregulated gene signatures shared between the diseases and *Shp*^{-/-} mice. Notably, several of the genes that showed significant differential expression in *Shp*^{-/-} mice and hepatitis C cirrhosis and/or NASH (Fig. 2, A–C) clustered together independently of any selection criteria. Interestingly, more genes appeared to be upregulated in cirrhosis vs. NASH livers, which partly reflects a greater change in liver

cell types in cirrhosis compared with NASH, which is an earlier stage of liver disease.

Heat maps of significantly differentially expressed genes in *Shp*^{-/-} mice compared with WT were produced from supervised

hierarchical clustering (Fig. 3B). This was also done for *Shp*^{-/-} mice and hepatitis C cirrhosis (Fig. 3C) and NASH (Fig. 3D) to highlight the shared DEGs with the most significant changes. The downregulated genes (*group 1*) (Fig. 3B) may represent genes



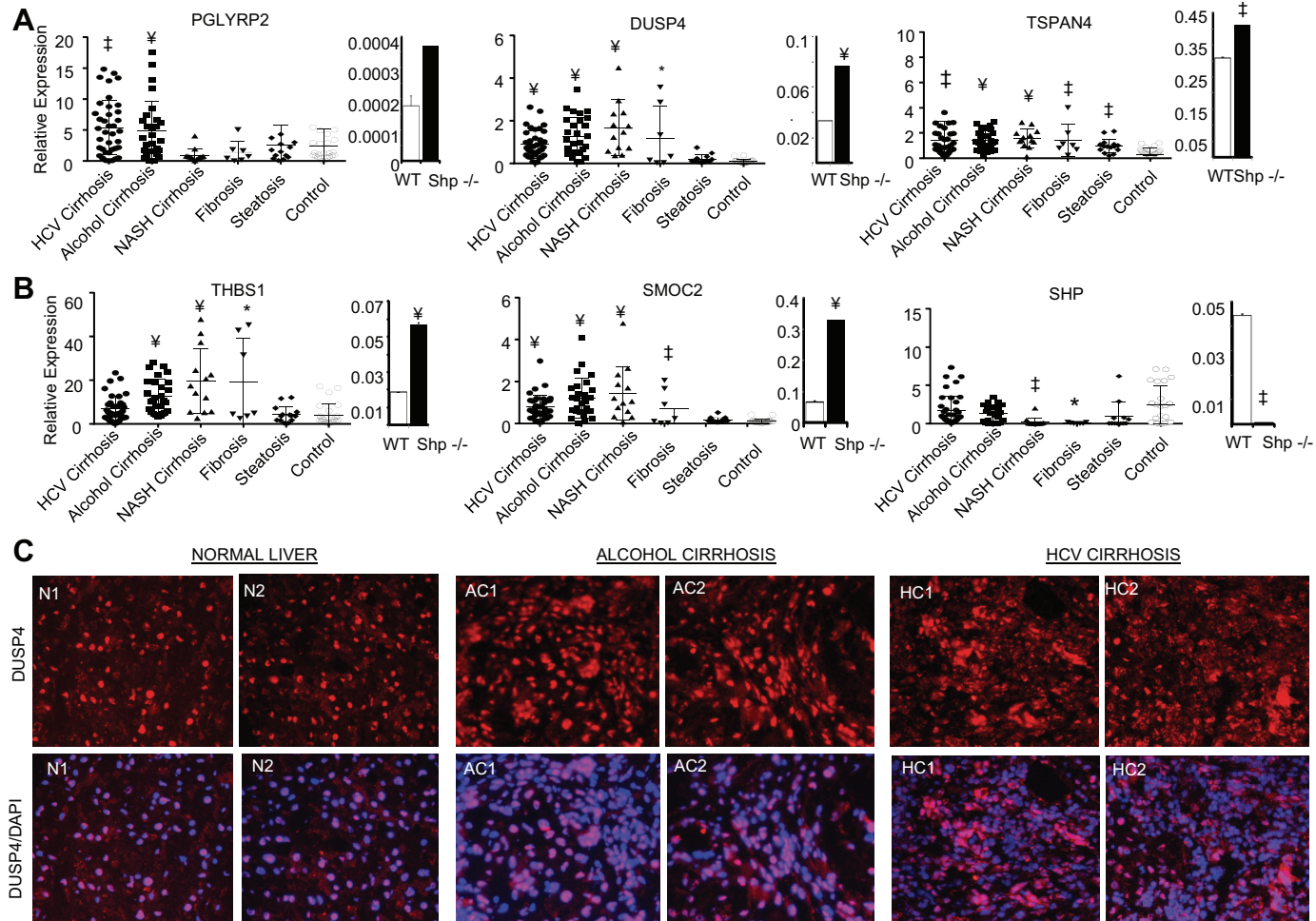


Fig. 4. qPCR validation of new genes that are differentially expressed in *Shp*^{-/-} mice, human liver steatosis, fibrosis, NASH, and alcohol and hepatitis C cirrhosis. *A*: from left to right, peptidoglycan recognition protein 2 (*PGLYRP2*), dual specific phosphatase-4 (*DUSP4*), and tetraspanin 4 (*TSPAN4*). *B*: from left to right, thrombospondin 1 (*THBS1*), SPARC-related modular calcium binding protein-2 (*SMOC2*), and SHP. Expression levels of each gene for each sample were normalized to the hypoxanthine phosphoribosyltransferase 1 expression level of that sample as an internal control. **P* < 0.001, †*P* < 0.01, and **P* < 0.05. The no. of specimens in each group is as follows: HCV cirrhosis (*n* = 39), alcohol cirrhosis (*n* = 28), NASH cirrhosis (*n* = 13), fibrosis (*n* = 7), steatosis (*n* = 15), and control (*n* = 24). *C*: immunohistochemistry analysis of *DUSP4* protein in human alcohol and hepatitis C cirrhosis compared with the normal liver. Two representative results from each group are shown. N, normal; AC, alcohol cirrhosis; HC, HCV cirrhosis. Top: *DUSP4* protein expression. Bottom: *DUSP4* overlay with DAPI staining. Magnification ×20.

silenced by hypermethylation when SHP repression of DNA methyltransferase 1 is released (45, 49). These genes could also be SHP transcriptional coregulators, or SHP-activated genes, such as peroxisome proliferator-activated receptor- γ (47). *Group 2* genes (Fig. 3*B*), those significantly upregulated in *Shp*^{-/-} mice, represented known and potential SHP direct or indirect targets for inhibition. *Groups 3* (Fig. 3*C*) and *5* (Fig. 3*D*) represented genes that are repressed in hepatitis C cirrhosis and NASH, respectively, and are a part of the SHP regulatory network. *Group 4* (Fig. 3*C*) and *6* (Fig. 3*D*) genes were also possible SHP targets such as

peptidoglycan recognition protein 2 (*PGLYRP2*). These cluster analyses provide a better visualization of changes in the gene expression pattern shared between the *Shp*^{-/-} mice and hepatitis C cirrhosis and/or NASH. Notably, there is more heterogeneity among the WT and control samples compared with the homogeneous gene expression pattern seen in *Shp*^{-/-} mice, hepatitis C cirrhosis, and NASH.

qPCR and IHC validation of selected genes in a large set of human liver specimens. *PGLYRP2*, *DUSP4*, tetraspanin 4 (*TSPAN4*), thrombospondin 1 (*THBS1*), and SPARC-related

Fig. 3. Hierarchical clustering of DEGs in *Shp*^{-/-} mice, chronic hepatitis C cirrhosis, and NASH. *A*: unsupervised hierarchical clustering of genes common to the NASH microarray and chronic hepatitis C cirrhosis and *Shp*^{-/-} RNA-seq gene expression arrays. *B*: heat map showing supervised hierarchical clustering of genes with fold changes in expression greater than or equal to ±5-fold in *Shp*^{-/-} compared with WT mice depicting potential SHP-activated genes in *group 1* and SHP-repressed genes in *group 2*. *C*: heat map showing supervised hierarchical clustering of selected genes with fold changes greater than or equal to ±1.5 in both cirrhotic compared with normal livers and in *Shp*^{-/-} compared with WT livers, demonstrating correlation between the disease state and *Shp*^{-/-} gene expression, those repressed in chronic hepatitis C cirrhosis in *group 3* and activated in *group 4*. *D*: similar to chronic hepatitis C cirrhosis, this heat map shows selected genes with fold changes greater than or equal to ±1.5-fold in NASH compared with normal livers common in *Shp*^{-/-} compared with WT livers and has a similar pattern.

modular calcium binding protein-2 (*SMOC2*) were highly differentially expressed and have barely characterized functions in liver disease. Intriguingly, our pathway analysis and literature search pointed to their possible involvement in liver disease. Therefore, we chose to further analyze these genes in a large set of human liver specimens, including normal liver, steatosis, fibrosis, NASH cirrhosis, alcohol cirrhosis, and hepatitis C cirrhosis. qPCR analysis showed that *PGLYRP2* expression was sharply increased in alcohol and hepatitis C cirrhosis and in *Shp*^{-/-} mice (Fig. 4A, left). *TSPAN4* (Fig. 4A, right), *THBS1* (Fig. 4B, left), and *SMOC-2* (Fig. 4B, middle) were all upregulated in fibrosis and cirrhosis. These genes also showed increased expression in *Shp*^{-/-} vs. WT mice. On the other hand, SHP levels were decreased in steatosis, fibrosis, and NASH cirrhosis, but not in hepatitis C cirrhosis (Fig. 4B, right).

Next, we chose to examine DUSP4 protein expression by IHC in human liver specimens. DUSP4 protein expression was much higher in alcohol and hepatitis C cirrhotic livers compared with normal livers (Fig. 4C), which is consistent with increased mRNA levels.

Functional significance of selected genes in mouse models of liver inflammation, fibrosis, and alcohol injury. To further confirm SHP regulation of the selected genes, we analyzed their expression levels in *Shp*^{-/-} and WT mice at different time points. Basal SHP mRNA levels exhibited diurnal fluctuation that was markedly higher at 24 h than at 6 h (Fig. 5A), consistent with SHP as a circadian clock-regulated gene (32, 46). The expression of *Pglyrp2*, *Dusp4*, *Thbs1*, and *Tspan4*

correlated negatively with SHP expression and so was higher at 6 h but lower at 24 h.

To provide initial evidence about the functional significance of the selected genes in liver inflammation, primary hepatocytes isolated from WT and *Shp*^{-/-} mice were subjected to LPS treatment. Interestingly, short-time LPS treatment (6 h) decreased *Pglyrp2*, *Dusp4*, *Thbs1*, and *Tspan4* mRNA in a dose-dependent fashion in the WT hepatocytes, but this effect of LPS was largely blockaded in *Shp*^{-/-} cells after 24 h (Fig. 5B). The levels of these genes were not further downregulated by LPS in WT cells at 24 h but were significantly induced in *Shp*^{-/-} cells (Fig. 5B). This indicates a derepression effect by the loss of SHP. Notably, the increased expression of *Pglyrp2* and *Dusp4* in *Shp*^{-/-} cells was enhanced by a high dose of LPS at 24 h.

Smoc2 exhibited a distinct expression profile. Its levels were not markedly altered by LPS in WT cells at 6 h but were highly induced in *Shp*^{-/-} cells regardless of the presence of LPS (Fig. 5B). Although *Smoc2* expression was ~50% reduced in *Shp*^{-/-} cells at 24 vs. 6 h, it was consistently high compared with WT cells. LPS treatment induced an approximately twofold increase in *Smoc2* expression in WT cells at 24 h.

We also investigated the relevance of these genes to bile acid injury using CCl₄- and DDC-induced mouse fibrosis models. *Pglyrp2* was induced by DDC but not by CCl₄ (Fig. 5C). *Dusp4* and *Tspan4* were induced by DDC and CCl₄, respectively, whereas *Thbs1* and *Smoc2* were markedly induced in both models.

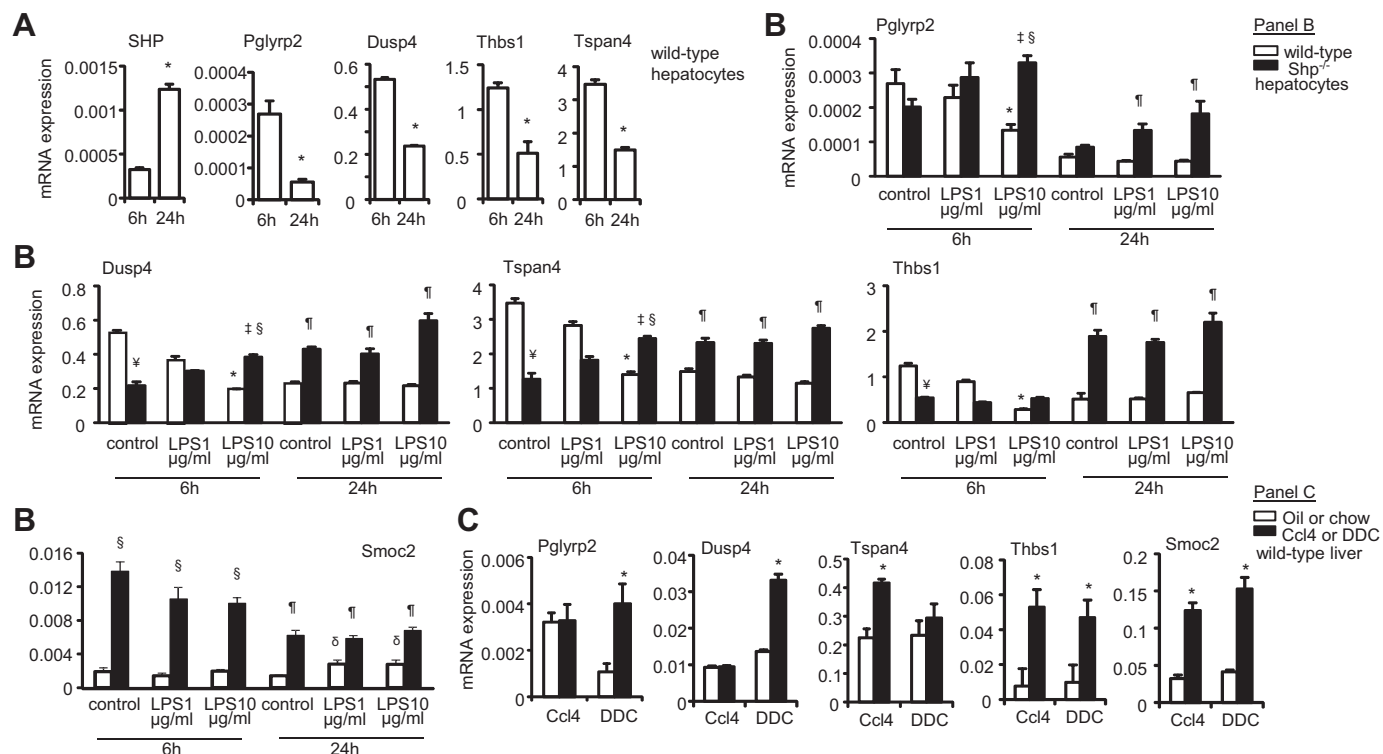


Fig. 5. Functional analysis of selected genes in mouse liver inflammatory and injury models. A: qPCR of gene expression in hepatocytes isolated from 2-mo-old male mice that were cultured for 6 and 24 h. *P < 0.01, 24 h vs. 6 h. B: qPCR of gene expression from WT and *Shp*^{-/-} hepatocytes treated with lipopolysaccharide (LPS) for 6 and 24 h. *P < 0.01, LPS 10 µg vs. LPS 1 µg or control in WT cells at 6 h; ‡P < 0.01, LPS 10 µg vs. control in *Shp*^{-/-} cells at 6 h; §P < 0.01, *Shp*^{-/-} vs. WT cells at 6 h; ¶P < 0.01, *Shp*^{-/-} vs. WT cells at 24 h; ¶P < 0.01, LPS vs. control at 24 h. C: qPCR of gene expression in mice fed with CCl₄ or 3,5-diethoxycarbonyl-1,4-dihydrocollidine (DDC) to induce liver fibrosis. *P < 0.01, CCl₄ or DDC vs. respective control.

SHP overexpression in Huh7 cells led to downregulation of Pglyrp2 and Thbs1 (Fig. 6A), whereas a moderate knockdown of SHP using RNAi led to upregulation of Thbs1 but not Pglyrp2 (Fig. 6B).

We next determined the expression of these genes in stellate (HSC) cells and their response to alcohol-induced liver injury. SHP was activated about 40-fold by alcohol, and Pglyrp2 was increased over 30-fold (Fig. 6D). Thbs1 and Tspan4 were induced three- and twofold, respectively (Fig. 6D).

*Multiple pathways are commonly altered in *Shp*^{-/-} mice, NASH, and hepatitis C cirrhosis.* Having identified shared gene signatures within the datasets, we then used the DAVID functional annotation tool to uncover multiple pathways shared between *Shp*^{-/-} mice and the liver diseases studied. We identified 171 GO pathways significantly enriched in *Shp*^{-/-} mice. Fifty four percent of these were also found in hepatitis C cirrhosis and 51% in NASH (Fig. 7, A and B). These were among the most highly enriched pathways in the hepatitis C cirrhosis DEG set, supporting the potential role of the identified genes in development of chronic liver disease. We also identified 18 KEGG pathways that were significantly altered in *Shp*^{-/-} mice, 44% of which were also enriched in hepatitis C cirrhosis and 50% were enriched in NASH (Fig. 7, A and B). *Pglyrp2*, *Dusp4*, *Tspan4*, *Thbs1*, and *Smoc2* were novel genes implicated in cellular oxidation, migration, adhesion, intracellular signaling, and inflammation pathways (Fig. 7C). This is the first report to show such a wide-ranging effect of SHP deficiency on multiple pathways, and we highlight specific

genes involved in physiological processes that are deregulated in major chronic liver diseases.

DISCUSSION

A revolution in the analysis of RNA has come through the development of deep sequencing technologies to map the entire transcriptome in cells and biospecimens (24, 25). Recently, this powerful approach revealed a comprehensive transcriptomic landscape in human HCC (17). However, such comprehensive RNA-seq analysis has not been performed in human liver NASH, fibrosis, or cirrhosis. In addition, establishing animal models that share common gene signatures with human liver diseases is essential to allow studies of genes important to human disease progression.

The present study is the first to conduct comparative RNA-seq analysis of human HCV cirrhosis specimens and *Shp*^{-/-} (*Nr0b2*^{-/-}) mice along with NASH gene array analysis. Thus, the results encompass several novel findings. The study revealed that SHP deficiency induced a significant shift in liver cellular metabolic and inflammatory states, and fibrogenic and oncogenic potential, which was also found in hepatitis C cirrhosis and NASH. Moreover, this study also identified new genes that are regulated by SHP and are differentially expressed during hepatic fibrosis and cirrhosis in humans. The findings are consistent with the role of SHP in regulating inflammatory response, lipid and xenobiotic metabolism, liver fibrogenesis, and oncogenesis (47) and suggests the dysregu-

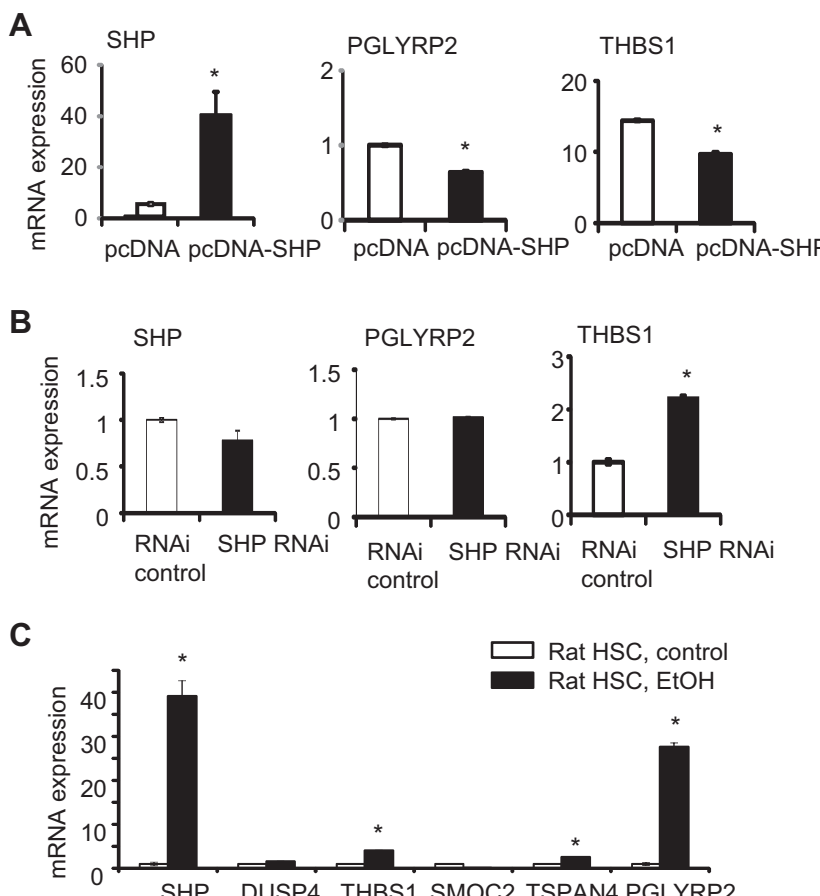
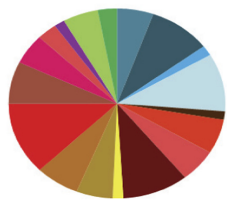


Fig. 6. Alteration in expression of selected genes in stellate cells from alcohol-induced liver injury. A and B: qPCR of gene expression in Huh7 cells with SHP overexpression (A) or knockdown (B). C: qPCR of gene expression in stellate cells [hepatic stellate cells (HSC)] isolated from alcohol-treated rats. *Significance was determined at $P < 0.01$.

A Upregulated in SHP -/- MiceAltered in SHP-/- Only

■ Fat cell differentiation

Altered in SHP-/- & HCV Cirrhosis

■ Regulation of catalytic activity

■ Growth and development

■ Actin based processes

■ Regulation of signal transduction, phosphorylation, JAK-STAT cascade

Altered in SHP-/- & NASH

■ RNA Pol II transcription and RNA stability

■ Modified lipid biosynthesis and metabolism

Altered in SHP-/-, HCV Cirrhosis & NASH

■ Protein processing and maturation

■ Lipid and isoprenoid homeostasis

■ Regulation of cell death and starvation response

■ Regulation of cell proliferation, migration and differentiation

■ Glycosylation

■ Inflammatory response and response to stimulus

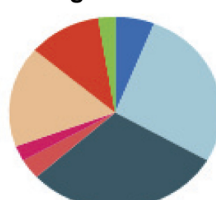
■ Oxidative phosphorylation, redox and energy generation

■ Molecular remodeling, transport and localization

■ Cellular homeostasis and response to stimulus

■ Amino acid and sulfur metabolism

■ Carbohydrate metabolism and response to carbohydrate stimulus

B Downregulated in SHP -/- MiceAltered in SHP-/- Only

■ regulation of lipase activity

■ artery morphogenesis

■ cell cycle

■ Positive regulation of catalytic activity

Altered in SHP-/- & HCV Cirrhosis

■ Positive regulation of kinase and transferase activity

■ Small GTPase signalling

■ oxidation reduction

Altered in SHP-/- & NASH

■ monocarboxylic acid transport

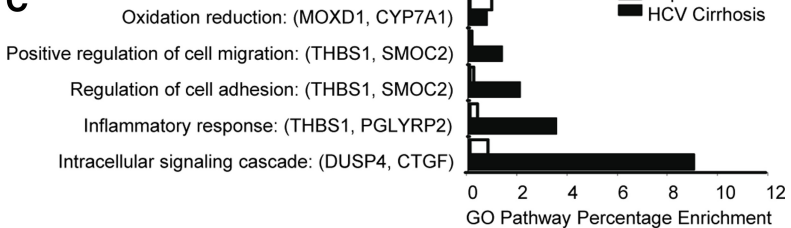
C

Fig. 7. Gene Ontology (GO) pathways enriched in *Shp*^{-/-} mice, HCV cirrhosis, and NASH. DEGs among *Shp*^{-/-} mice, HCV cirrhosis, and NASH datasets were fed into the Database for Annotation, Visualization, and Integrated Discovery (DAVID) version 6.7 functional annotation software and used to generate GO pathways enriched in our gene sets. Pathways enriched in genes upregulated (A) and downregulated (B) in *Shp*^{-/-} mice and altered in HCV cirrhosis and NASH are shown. Pie chart slices represent the numbers of DEGs listed in each pathway. Significance was determined at $P < 0.05$. C: GO pathway analysis of DEGs in both human hepatitis C cirrhosis and *Shp*^{-/-} mouse showing several highly enriched pathways and the percentage enrichment of these pathways (significance of $P < 0.05$). Two notable genes in each pathway are shown in parentheses.

lution of SHP participates in the biology of human chronic liver diseases. The overlap of genes we have found between murine and human conditions is suggested to represent critical gene expression changes in the progression or development of liver disease. Each disease condition, both mouse and human, arose from varying insults and early genomic changes, but they likely converge to disease development and/or progression through similar critical pathways. Our RNA-seq analysis has recapitulated known gene expression changes involved in chronic liver disease, such as increase in CYP7A1 and EGR1 expression, and we now present novel genes that are similarly implicated. The specific causal and/or functional roles of these genes will be thoroughly investigated in future studies.

The genes we selected for validation were all significantly upregulated in *Shp*^{-/-} mice, hepatitis C cirrhosis, and/or NASH and formed a part of the shared signatures created by hierarchical clustering analysis. Additionally, they were identified in inflammatory response, cell migration, or adhesion pathways, or their involvement in liver disease was suggested in the literature.

PGLYRP2, which was upregulated in hepatitis C and alcohol cirrhosis biospecimens, belongs to an innate immunity protein family expressed in the liver (8) and was identified in the early inflammatory response of the gut in mice with colitis (37). Other genes were upregulated in *Shp*^{-/-} mice and all fibrotic liver disease biospecimens, i.e., fibrosis and NASH, alcohol and hepatitis C cirrhosis. *DUSP4* is a MAPK phosphatase (20) whose methylation was significantly correlated with recurrence-free survival in hepatitis C-induced HCC (7). *TSPAN4* and *Smoc2* were also upregulated in *Shp*^{-/-} mice and fibrotic liver disease. A recent study showed that *TSPAN4* was significantly overexpressed in HCC (22), and *Smoc2* potentiates the angiogenic effects of growth factors (35). However, the functions of these genes in liver remain largely unstudied.

The marked increase of these genes in the fibrotic liver disease biospecimens, as well as in CCl₄- and DDC-induced liver fibrosis in mice, suggests they are involved in the pathogenesis of fibrotic liver diseases in humans. Interestingly, *Pglyrp2*, *Dusp4*, *Tspan4*, and *Thbs1* expression is decreased by SHP, and LPS does not increase their expression in WT

hepatocytes. However, with SHP deficiency, as is found with fibrotic liver diseases in our study, expression of *Pylrp2*, *Dusp4*, and *Tspan4* is induced and further increased on LPS treatment. *THBS1* was previously implicated in congenital hepatic fibrosis (9), and its expression was gradually increased with the severity of fibrosis induced by diethyl nitrosamine in rats (10). Our results are consistent with this hypothesis. *THBS1* mRNA was increased with CCl₄- and DDC-induced fibrosis in our mouse models and in the majority of fibrotic liver biospecimens, providing evidence that it is likely to be involved in human fibrotic liver disease.

SHP is most abundantly expressed in hepatocytes; therefore, the current study focused mostly on investigating that cell type. Intriguingly, our study for the first time revealed that SHP exhibited distinct and striking responses to alcohol-induced liver injury in nonparenchymal cells; it was highly activated in stellate cells by alcohol. The alteration in its gene expression in this cell population may explain why SHP levels were not downregulated in alcohol cirrhosis as seen in steatosis, when total liver mRNA was examined. Interestingly, induction of SHP in a rat bile duct ligation model of liver fibrosis inhibited stellate cell function and protected against liver fibrosis (11). It remains to be determined whether posttranslational modifications, such as ubiquitination (51), or pathways through other nuclear receptors contribute to SHP expression in alcohol and HCV cirrhosis. In addition, how alcohol and HCV affect SHP levels in Kupffer cells needs to be investigated. On the other hand, the cell type-specific response to alcohol of *Pglyrp2*, and to a lesser extent *Thbs1* and *Tspan4* in stellate cells, suggests vital roles for these genes in alcohol-induced liver injury through to cirrhosis. In HSC cells, *Pglyrp2* may be regulated in a SHP-independent manner.

In summary, our study provides new hypotheses regarding the molecular basis of chronic liver diseases in humans. The newly described genes that are similarly altered in *Shp*^{-/-} mice and chronic liver disease highlight the need for further studies of the possible mechanistic role of these genes in hepatic fibrogenesis and chronic liver disease in both patients and model systems such as *Shp*^{-/-} mice.

ACKNOWLEDGMENTS

We thank Drs. David Nix and Brian Dalley from the Microarray and Genomic Analysis Core Facility at the University of Utah for assistance with the RNA sequencing analysis.

GRANTS

The human liver specimens were obtained through the Liver Tissue Cell Distribution System (Minneapolis, MN), which is funded by National Institutes of Health Contract No. N01-DK-7-0004/HHSN267200700004C. This work was supported by the National Institutes of Health (DK-080440 to L. Wang and CA-148068 to C. Hagedorn).

DISCLOSURES

No conflicts of interest, financial or otherwise, are declared by the authors.

AUTHOR CONTRIBUTIONS

Author contributions: R.S., D.D., C.H., and L.W. conception and design of research; R.S., Y.Z., N.N., and S.L. performed experiments; R.S., D.D., Y.Z., M.S.M., C.H., and L.W. analyzed data; R.S., D.D., Y.Z., C.H., and L.W. interpreted results of experiments; R.S., M.S.M., and L.W. prepared figures; R.S. drafted manuscript; R.S., D.D., Y.Z., N.N., S.L.F., C.H., and L.W. edited and revised manuscript; R.S., D.D., Y.Z., C.H., and L.W. approved final version of manuscript.

REFERENCES

1. Aktas B, Yilmaz Y, Eren F, Yonal O, Kurt R, Alahdab YO, Celikel CA, Ozdogan O, Imeryuz N, Kalayci C, Avsar E. Serum levels of vaspin, obestatin, and apelin-36 in patients with nonalcoholic fatty liver disease. *Metab Clin Exp* 60: 544–549, 2011.
2. Baker SS, Baker RD, Liu W, Nowak NJ, Zhu L. Role of alcohol metabolism in non-alcoholic steatohepatitis. *PLoS One* 5: e9570, 2010.
3. Brunt EM. Nonalcoholic steatohepatitis. *Semin Liver Dis* 24: 3–20, 2004.
4. Choi YH, Hagedorn CH. Purifying mRNAs with high-affinity eIF4E mutant identifies the short 3' poly(A) end phenotype. *Proc Natl Acad Sci USA* 100: 7033–7038, 2003.
5. Cubero FJ, Nieto N. Ethanol and arachidonic acid synergize to activate Kupffer cells and modulate the fibrogenic response via tumor necrosis factor alpha, reduced glutathione, and transforming growth factor beta-dependent mechanisms. *Hepatology* 48: 2027–2039, 2008.
6. Datta S, Wang L, Moore DD, Osborne TF. Regulation of 3-hydroxy-3-methylglutaryl coenzyme A reductase promoter by nuclear receptors liver receptor homologue-1 and small heterodimer partner: a mechanism for differential regulation of cholesterol synthesis and uptake. *J Biol Chem* 281: 807–812, 2006.
7. Deng YB, Nagae G, Midorikawa Y, Yagi K, Tsutsumi S, Yamamoto S, Hasegawa K, Kokudo N, Aburatani H, Kaneda A. Identification of genes preferentially methylated in hepatitis C virus-related hepatocellular carcinoma. *Cancer Sci* 101: 1501–1510, 2010.
8. Dziarski R, Gupta D. Mammalian peptidoglycan recognition proteins (PGRPs) in innate immunity. *Innate Immunity* 16: 168–174, 2010.
9. El-Youssef M, Mu Y, Huang L, Stellmach V, Crawford SE. Increased expression of transforming growth factor-beta1 and thrombospondin-1 in congenital hepatic fibrosis: possible role of the hepatic stellate cell. *J Pediatr Gastroenterol Nutr* 28: 386–392, 1999.
10. Elpek GO, Gokhan GA, Bozova S. Thrombospondin-1 expression correlates with angiogenesis in experimental cirrhosis. *World J Gastroenterol* 14: 2213–2217, 2008.
11. Fiorucci S, Antonelli E, Rizzo G, Renga B, Mencarelli A, Riccardi L, Orlandi S, Pellicciari R, Morelli A. The nuclear receptor SHP mediates inhibition of hepatic stellate cells by FXR and protects against liver fibrosis. *Gastroenterology* 127: 1497–1512, 2004.
12. He N, Park K, Zhang Y, Huang J, Lu S, Wang L. Epigenetic inhibition of nuclear receptor small heterodimer partner is associated with and regulates hepatocellular carcinoma growth. *Gastroenterology* 134: 793–802, 2008.
13. Huang da W, Sherman BT, Lempicki RA. Bioinformatics enrichment tools: paths toward the comprehensive functional analysis of large gene lists. *Nucleic Acids Res* 37: 1–13, 2009.
14. Huang da W, Sherman BT, Lempicki RA. Systematic and integrative analysis of large gene lists using DAVID bioinformatics resources. *Nature Prot* 4: 44–57, 2009.
15. Huang J, Iqbal J, Saha PK, Liu J, Chan L, Hussain MM, Moore DD, Wang L. Molecular characterization of the role of orphan receptor small heterodimer partner in development of fatty liver. *Hepatology* 46: 147–157, 2007.
16. Huang J, Tabbi-Anneni I, Gunda V, Wang L. Transcription factor Nrf2 regulates SHP and lipogenic gene expression in hepatic lipid metabolism. *Am J Physiol Gastrointest Liver Physiol* 299: G1211–G1221, 2010.
17. Huang Q, Lin B, Liu H, Ma X, Mo F, Yu W, Li L, Li H, Tian T, Wu D, Shen F, Xing J, Chen ZN. RNA-Seq analyses generate comprehensive transcriptomic landscape and reveal complex transcript patterns in hepatocellular carcinoma. *PLoS One* 6: e26168, 2011.
18. Jeschke MG, Klein D, Thasler WE, Bolder U, Schlitt HJ, Jauch KW, Weiss TS. Insulin decreases inflammatory signal transcription factor expression in primary human liver cells after LPS challenge. *Mol Med* 14: 11–19, 2008.
19. Jin T, Xu D, Ding Q, Zhang Y, Mao C, Pan Y, Wang Z, Chen Y. Identification of the topology and functional domains of PAQR10. *Biochem J* 443: 643–653, 2012.
20. Keyse SM. Dual-specificity MAP kinase phosphatases (MKPs) and cancer. *Cancer Metastasis Rev* 27: 253–261, 2008.
21. Kirby GM, Nichols KD, Antenos M. CYP2A5 induction and hepatocellular stress: an adaptive response to perturbations of heme homeostasis. *Curr Drug Metab* 12: 186–197, 2011.
22. Li Y, Wang L, Qiu J, Da L, Tiollais P, Li Z, Zhao M. Human tetraspanin transmembrane 4 superfamily member 4 or intestinal and liver tetraspan membrane protein is overexpressed in hepatocellular carcinoma

- and accelerates tumor cell growth. *Acta Biochim Biophys Sinica* 44: 224–232, 2012.
23. Lieber CS, DeCarli LM, Sorrell MF. Experimental methods of ethanol administration. *Hepatology* 10: 501–510, 1989.
 24. Malone JH, Oliver B. Microarrays, deep sequencing and the true measure of the transcriptome (Abstract). *BMC Biol* 9: 34, 2011.
 25. Martin JA, Wang Z. Next-generation transcriptome assembly. *Nat Rev Genet* 12: 671–682, 2011.
 26. Matsukuma KE, Bennett MK, Huang J, Wang L, Gil G, Osborne TF. Coordinated control of bile acids and lipogenesis through FXR-dependent regulation of fatty acid synthase. *J Lipid Res* 47: 2754–2761, 2006.
 27. Matsukuma KE, Wang L, Bennett MK, Osborne TF. A key role for orphan nuclear receptor liver receptor homologue-1 in activation of fatty acid synthase promoter by liver X receptor. *J Biol Chem* 282: 20164–20171, 2007.
 28. Miele L, Forgione A, Hernandez AP, Gabrieli ML, Vero V, Di Rocco P, Greco AV, Gasbarrini G, Gasbarrini A, Grieco A. The natural history and risk factors for progression of non-alcoholic fatty liver disease and steatohepatitis. *Eur Rev Med Pharmacol Sci* 9: 273–277, 2005.
 29. Nix DA, Courdy SJ, Boucher KM. Empirical methods for controlling false positives and estimating confidence in ChIP-Seq peaks (Abstract). *BMC Bioinformatics* 9: 523, 2008.
 30. Oler AJ, Alla RK, Roberts DN, Wong A, Hollenhorst PC, Chandler KJ, Cassiday PA, Nelson CA, Hagedorn CH, Graves BJ, Cairns BR. Human RNA polymerase III transcriptomes and relationships to Pol II promoter chromatin and enhancer-binding factors. *Nat Struct Mol Biol* 17: 620–628, 2010.
 31. Ondracek CR, Reese VC, Rushing CN, Oropeza CE, McLachlan A. Distinct regulation of hepatitis B virus biosynthesis by peroxisome proliferator-activated receptor gamma coactivator 1alpha and small heterodimer partner in human hepatoma cell lines. *J Virol* 83: 12545–12551, 2009.
 32. Pan X, Zhang Y, Wang L, Hussain MM. Diurnal regulation of MTP and plasma triglyceride by CLOCK is mediated by SHP. *Cell Metab* 12: 174–186, 2010.
 33. Papic N, Maxwell CI, Delker DA, Liu S, Heale BS, Hagedorn CH. RNA-sequencing analysis of 5' capped RNAs identifies many new differentially expressed genes in acute hepatitis C virus infection. *Viruses* 4: 581–612, 2012.
 34. Park YJ, Qatanani M, Chua SS, LaRey JL, Johnson SA, Watanabe M, Moore DD, Lee YK. Loss of orphan receptor small heterodimer partner sensitizes mice to liver injury from obstructive cholestasis. *Hepatology* 47: 1578–1586, 2008.
 35. Rocnik EF, Liu P, Sato K, Walsh K, Vaziri C. The novel SPARC family member SMOC-2 potentiates angiogenic growth factor activity. *J Biol Chem* 281: 22855–22864, 2006.
 36. Ruffalo M, LaFramboise T, Koyuturk M. Comparative analysis of algorithms for next-generation sequencing read alignment. *Bioinformatics* 27: 2790–2796, 2011.
 37. Saha S, Jing X, Park SY, Wang S, Li X, Gupta D, Dziarski R. Peptidoglycan recognition proteins protect mice from experimental colitis by promoting normal gut flora and preventing induction of interferon-gamma. *Cell Host Microbe* 8: 147–162, 2010.
 38. Scholtes C, Diaz O, Icard V, Kaul A, Bartenschlager R, Lotteau V, Andre P. Enhancement of genotype 1 hepatitis C virus replication by bile acids through FXR. *J Hepatol* 48: 192–199, 2008.
 39. Starley BQ, Calcagno CJ, Harrison SA. Nonalcoholic fatty liver disease and hepatocellular carcinoma: a weighty connection. *Hepatology* 51: 1820–1832, 2010.
 40. Tiniakos DG, Vos MB, Brunt EM. Nonalcoholic fatty liver disease: pathology and pathogenesis. *Ann Rev Pathol* 5: 145–171, 2010.
 41. Wang L, Han Y, Kim CS, Lee YK, Moore DD. Resistance of SHP-null mice to bile acid-induced liver damage. *J Biol Chem* 278: 44475–44481, 2003.
 42. Wang L, Lee YK, Bundman D, Han Y, Thevananther S, Kim CS, Chua SS, Wei P, Heyman RA, Karin M, Moore DD. Redundant pathways for negative feedback regulation of bile acid production. *Dev Cell* 2: 721–731, 2002.
 43. Wang YD, Chen WD, Moore DD, Huang W. FXR: a metabolic regulator and cell protector. *Cell Res* 18: 1087–1095, 2008.
 44. Zhang DY, Friedman SL. Fibrosis-dependent mechanisms of hepatocarcinogenesis. *Hepatology* 56: 769–775, 2012.
 45. Zhang Y, Andrews GK, Wang L. Zinc-induced Dnmt1 expression involves antagonism between MTF-1 and nuclear receptor SHP. *Nucleic Acids Res* 40: 4850–4860, 2012.
 46. Zhang Y, Bonzo JA, Gonzalez FJ, Wang L. Diurnal regulation of the early growth response 1 (Egr-1) protein expression by hepatocyte nuclear factor 4alpha (HNF4alpha) and small heterodimer partner (SHP) cross-talk in liver fibrosis. *J Biol Chem* 286: 29635–29643, 2011.
 47. Zhang Y, Hagedorn CH, Wang L. Role of nuclear receptor SHP in metabolism and cancer. *Biochim Biophys Acta* 1812: 893–908, 2011.
 48. Zhang Y, Soto J, Park K, Viswanath G, Kuwada S, Abel ED, Wang L. Nuclear receptor SHP, a death receptor that targets mitochondria, induces apoptosis and inhibits tumor growth. *Mol Cell Biol* 30: 1341–1356, 2010.
 49. Zhang Y, Wang L. Nuclear receptor SHP inhibition of Dnmt1 expression via ERRgamma. *FEBS Lett* 585: 1269–1275, 2011.
 50. Zhang Y, Xu P, Park K, Choi Y, Moore DD, Wang L. Orphan receptor small heterodimer partner suppresses tumorigenesis by modulating cyclin D1 expression and cellular proliferation. *Hepatology* 48: 289–298, 2008.
 51. Zhou T, Zhang Y, Macchiarulo A, Yang Z, Cellanetti M, Coto E, Xu P, Pellicciari R, Wang L. Novel polymorphisms of nuclear receptor SHP associated with functional and structural changes. *J Biol Chem* 285: 24871–24881, 2010.